CHAPTER 74

GENERATION OF INFRAGRAVITY WAVES IN BREAKING PROCESS OF WAVE GROUPS

Satoshi NAKAMURA[1] and Kazumasa KATOH[1]

Abstract

To understand the cross-shore distribution of the wave groups and the infragravity waves in a storm, field observations have been carried out at the Hazaki Oceanographical Research Facility. The relationship between the wave groups and the infragravity waves is examined. The infragravity waves are generated in the wave breaking process of the wave groups. The observed heights of infragravity waves in the surf zone agree well with the predicted one by modified Symonds' model, in which a time delay of small wave breaking due to propagation is taken into consideration.

1 Introduction

Infragravity waves have been considered to be the main cause of abrupt beach erosion in a storm. For example, Katoh *et al.*(1990,1992) reported the field evidences of foreshore erosion due to the infragravity waves in the storms. Then, to predict the extent of abrupt beach erosions and to develop the effective countermeasures for them, it is important to estimate the magnitude of infragravity waves in a storm.

Although sea waves may look random, inspection of wave records indicates that high waves fall into groups rather than appear individually. This is called a wave groups. Concerning to the generation mechanism of infragravity waves, Symonds *et al.*(1982) showed the attractive theory by taking the wave groups into account. Nearly 10 years, however, have passed in a situation that their theory has not been verified with the field data.

The first purpose of this study is to carry out the simultaneous observation of the cross-shore changes of the wave groups and the infragravity waves in the storm, in order to understand their actual conditions. The secondary one is to modify the theory under ceratin circumstances for developing the more precise predictive model of infragravity waves in the surf zone.

[1]Port and Harbour Res. Inst., 3-1-1, Nagase, Yokosuka, Kanagawa, Japan

2 Field observations

2.1 Study site and method of observations

The site of field observations is a entirely natural sandy beach, being exposed to the full wave energy of the Pacific Ocean. On this beach, Port and Harbour Research Institute constructed the Hazaki Oceanographical Research Facility(HORF) for carrying out field observations in the surf zone under storm conditions(see Photo.1). A sediment research pier is 427 meters long.

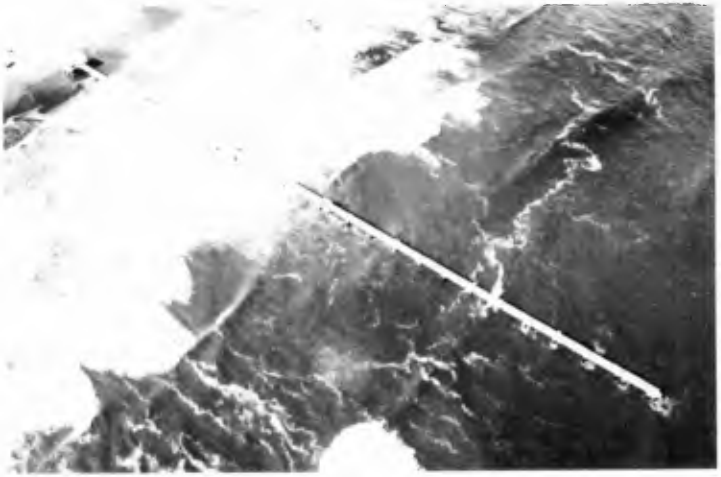

Photo. 1 Hazaki Oceanographical Research Facility(HORF).

Figure 1 shows the sea bottom profile and the locations where wave gages were set. Seven wave gages are permanently installed on the side of pier deck at the locations from No.1 to No.7 along the research pier. They emit supersonic waves downward and receive the supersonic waves reflected by the sea surface. At each location, wave profiles were measured continuously with a sampling time of 0.5 second. The data were sent to the laboratory at the base of research pier, where

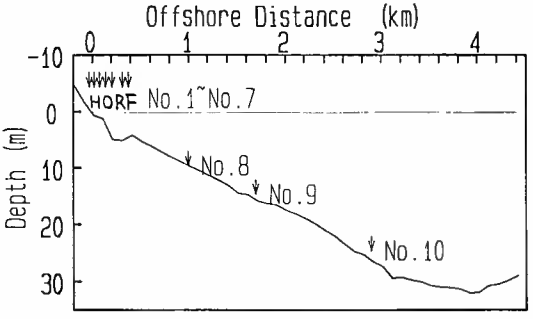

Figure 1 Beach profile and locations of measurement.

the signals were digitalized by a mini-computer and recorded on MT.

The other three wave gages at the locations from No.8 to No.10 were temporarily set on the sea bottom during storm, which were on the extension line of the pier. The water depths at these observation points were 9 meters, 14 meters and 24 meters respectively. At each location, waves were measured during 2 hours of every 6 hours with a sampling time of 0.5 second. The data were stored in a data cassette or an IC memory.

2.2 Wave conditions

The field observations were repeatedly carried out in the two different types of storm. Figure 2 shows the changes of offshore significant wave heights and periods, during the first observation from the 25th February to the 1st March in 1989. The maximum peak of wave height was 3.7 meters on the 26th February,

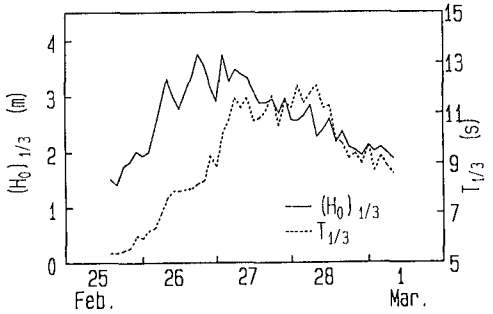

Figure 2 Changes of significant wave height and period in the first observation.

when the atmospheric depression passed through near the site. Figure 3 shows wave heights and periods during the second observation from the 5th to the 9th October in 1989. The maximum wave height was 4.6 meters on the 8th October, when the typhoon passed near the site.

Twenty-nine sets of ten wave records obtained during these two storms have been analyzed in this study. Figure 4 shows the cross-shore distribution of the spectral energy densities in two hours, when the significant wave height was 3.7

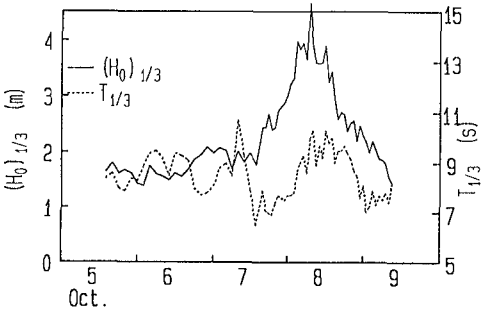

Figure 3 Changes of significant wave height and period in the second observation.

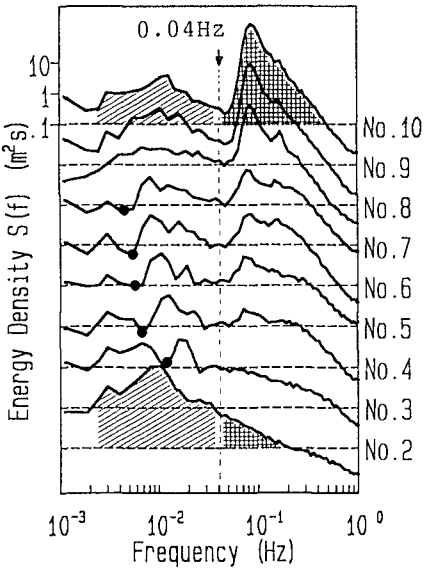

Figure 4 Cross-shore distribution of spectral energy densities.

meters in the offshore. The spectral energy density at the location of No.10 has two peaks. The first largest peak is at 0.1 Hz in frequency and second one is at 0.01 Hz. In addition, there is the minimum spectral density at the frequency of 0.04 Hz. The energy densities higher than 0.04 Hz in frequency are due to the incident wind waves, while those lower than 0.04Hz are considered to be due to the infragravity waves. The former decreases due to the wave breaking with propagation to the shoreline in the surf zone, while the latter increases in the onshore direction. The height, H_L, and period, T_L, of infragravity waves have been estimated by calculating the 0th-order and 2nd-order moments of the spectral energy density in the frequency band from 0 to 0.04Hz as follows;

$$H_L = 4 \int_0^{0.04} S(f) df, \tag{1}$$

$$T_L = \frac{\sqrt{\int_0^{0.04} S(f) df}}{\sqrt{\int_0^{0.04} f^2 S(f) df}}. \tag{2}$$

3 Data analysis on wave groups

3.1 Analysis of wave groups

A new method has been introduced for analyzing the wave groups, which can be applied to irregular waves trains both in the offshore and in the surf zone. The new method of analysis is explained in Figure 5, by using the wave profile data measured in the surf zone. First of all, the low frequency components less than

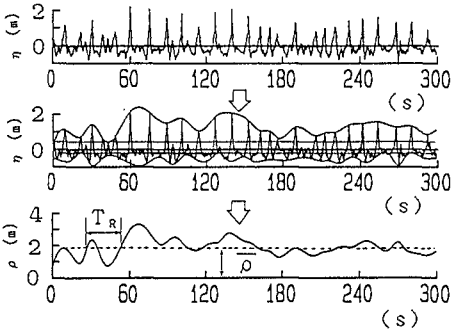

Figure 5 Method of wave groups analysis.

0.04Hz have been removed by using a numerical filter. The upper in Figure 5 is a high-pass-filtered wave profile. There are many small waves which are due to wave breaking and the non-lineality of waves. If individual waves are defined by the usual zero-crossing method, a wave number is greater in the surf zone than in the offshore. For removing small waves, a certain narrow band is established around the mean water level as shown in the middle of Figure 5. The small waves, whose wave height are less than the width of band, are neglected. The width of band has been determined so as to have the same wave number as that in the offshore.

After that, a natural cubic spline curve is fitted on each train of wave crests and wave troughs respectively. As the vertical width between the upper and the lower envelop curves corresponds to the wave height, the continuous wave height, $\rho(t)$, can be calculated as shown in the lower.

Based on this results, a mean wave height, $\bar{\rho}$, and a mean deviation around the mean wave height, ρ_{rms}, can be easily calculated by the following equations.

$$\bar{\rho} = \frac{1}{T_n}\int_0^{T_n} \rho(t)dt, \tag{3}$$

$$\rho_{rms} = \sqrt{\frac{1}{T_n}\int_0^{Tn} (\rho(t) - \bar{\rho})^2 dt}, \tag{4}$$

where T_n is total length of wave record.

If we adopt the Rayleigh distribution as the distribution of wave heights, the probability density function of $\rho(t)$ is written as

$$p(x) = \frac{\pi}{2} x \exp(-\frac{\pi}{4}x^2) \ : x = \rho/\bar{\rho}. \tag{5}$$

By utilizing Eq.(5) and conducting a numerical integration, Eq.(4) can be rewritten as

$$\rho_{rms} = \bar{\rho}\sqrt{\int_0^{\infty} (1-x)^2 p(x)dx} = 0.52\bar{\rho}. \tag{6}$$

There is a well-known relation between $H_{1/3}$ and $\bar{H}$(Goda,1985), that is

$$H_{1/3} = 1.60\bar{H}(= 1.60\bar{\rho}). \tag{7}$$

By substituting Eq.(7) into Eq.(6),

$$\rho_{rms} \doteq \frac{1}{3}H_{1/3}. \tag{8}$$

Figure 6 shows the comparison of ρ_{rms} with $H_{1/3}$ in the offshore. The data are plotted close to the dashed line which is the theoretical relation of Eq.(8).

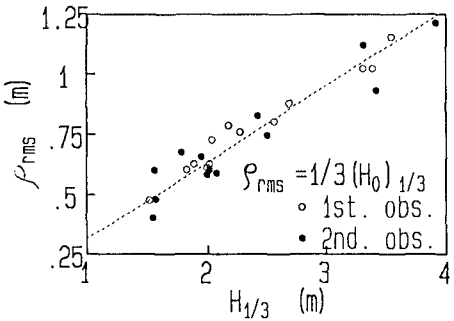

Figure 6 Comparison of ρ_{rms} with $H_{1/3}$.

A repetition period of wave groups is defined as an elapsed time from the time that wave height is excess of a threshold value to the time of its re-excess, that is to say, in the same manner as what is called a zero-crossing method. The individual repetition period of the wave groups and its mean value are denoted by T_R and $\bar{T}_R$, respectively, hereinafter. Several calculations of the mean repetition period, $\bar{T}_R$, have been done by changing the threshold value. Comparing the calculated mean repetition period in the offshore with the observed period of infragravity waves in the surf zone, it has been confirmed that the former agrees approximately with the latter when a highest one-tenth wave, $H_{1/10}$, is used as the threshold height. Figure 7 shows the histogram of the repetition periods of wave groups at the offshore in one record length of 2 hours when the significant wind wave height was 3.7 meters. The repetition periods of 60 wave groups are distributed in a wide range. Although there is no predominant peak of frequency in the distribution, the mean repetition period of $\bar{T}_R$ is used as the representative value for convenience. Figure 8 shows a comparison of the mean repetition period of the wave groups with the significant wave period at the point of No.10. By means of the least square method, the increasing tendency of T_R can be expressed as

$$\bar{T}_R = 9.24T_{1/3}. \tag{9}$$

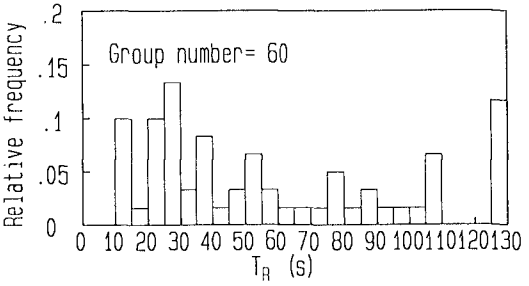

Figure 7 Histogram of repetition period.

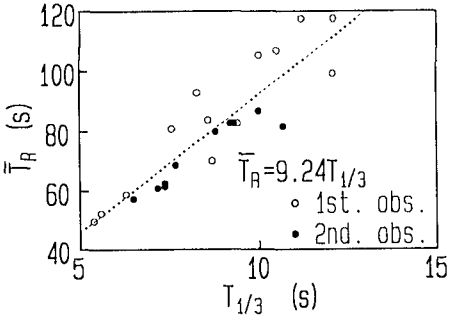

Figure 8 Comparison of significant wave period with mean repetition period.

3.2 Relationship between wave groups and infragravity waves

Figure 9 shows the cross-shore distribution of the mean repetition period of wave groups, $\bar{T}_R$, and the height of the infragravity waves, H_L, when the significant wave height was 3.7 meters. The mean repetition period of the wave groups decreased rapidly near the point of No.8, where the height of the infragravity waves increased. According to our visual observation, the incident wind waves broke in the area between the points of No.7 and 8. On the other hand, when the significant wave height was 1.8 meters in the offshore, which is not shown here,

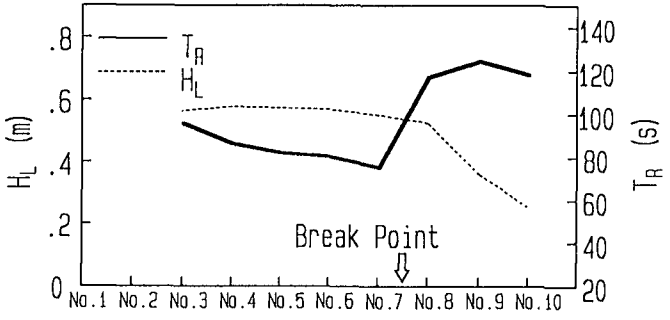

Figure 9 Distribution of $\bar{T}_R$ and H_L in the storm.

the mean repetition period of the wave groups was not long in the offshore, and the height of infragravity wave increased slightly, being still small in the surf zone. Then, it is inferred from these evidence that infragravity waves are generated in the wave breaking process when the mean repetition period of wave groups is long.

4 Modification of Symonds' model

4.1 Applicability of Symonds' model

Symonds *et al.*(1982) showed that the time variation of the break point, which occurs when the incident waves are of varying amplitude, can generate waves at the group period and may be a significant source of infragravity wave energy. They used the non-dimensional, depth-integrated and linearized shallow water equations, that is,

$$\chi \frac{\partial U}{\partial t} + \frac{\partial \zeta}{\partial x} = -F(x,t), \tag{10}$$

$$\frac{\partial \zeta}{\partial t} + \frac{\partial (xU)}{\partial x} = 0, \tag{11}$$

$$\chi = \frac{\sigma^2 X}{g \tan\beta}, \quad \sigma = \frac{2\pi}{T_R}, \quad x = \frac{x'}{X}, \quad t = t'\sigma$$

where x' is a distance with the origin at the shoreline, ζ is the sea surface, U is the depth-integrated velocity, a is the incident wave amplitude, X is the mean position of the break point, $\tan\beta$ is the beach slope and g is the gravitational acceleration.

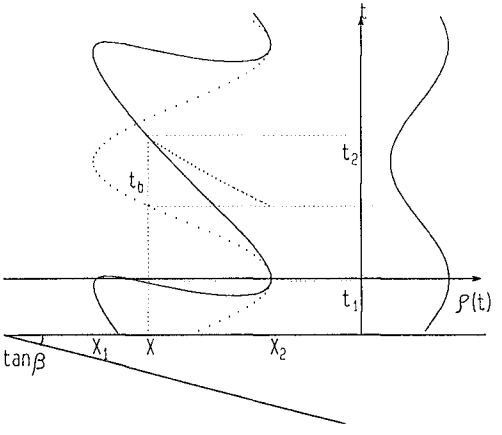

Figure 10 Schematic representation of Symonds' model.

To solve these equations, it is necessary to determine an analytic form for the forcing term on the right-hand side of Eq.(10). The value of the forcing term

depends on the position of the breakpoint, $x_b(t)$,

$$F(x,t) = \frac{1}{2x}\frac{\partial(a^2)}{\partial x} = \begin{cases} 1 & x < x_b(t) \\ 0 & x > x_b(t) \end{cases} \tag{12}$$

The duration of the pulse of Eq.(12) is a function of x. For x located from x_1 to x_2, the forcing term, F, defined by Eq.(12) tend to a series of pulses. For x located from 0 to x_1, it is unity for all time. Otherwise, it is zero for all time.

In the analytical treatment, after considering the result of pre-calculation in two cases of χ from 1 to 5, Symonds *et al.* neglected the travel time, t_b. Then, by assuming that the break point varies sinusoidally with time as shown with the dotted line in Figure 10, they derived the analytical solution of the infragravity waves. By using the Symonds' model, the heights of infragravity waves in the surf zone had been calculated with the field data. In this calculation, we made some assumptions as follows:

a) Although there is the wide distribution of repetition periods as shown in Figure 7, the amplitude of incident waves varies sinusoidally with the observed mean repetition period of wave groups, that is,

$$\rho(t) = \bar{\rho} + \sqrt{2}\rho_{rms}\cos(\frac{2\pi}{\bar{T}_R}t). \tag{13}$$

b) The slope of the bottom profile is constant, being $\tan\beta = 1/140$ which is a mean slope around wave breaking points in the storms.

c) The wave breaking point is determined as the appearance point of the peak value of significant waves, employing the Goda's breaker indices(Goda,1985).

Figure 11 shows the comparison of the predicted height of infragravity waves with the observed one, where the dotted line indicates the relation of coincidence between them. The height of infragravity waves is defined as the mean value of the heights at the observation points in the surf zone. The predicted heights are about four times as large as observed ones. The large difference between them has

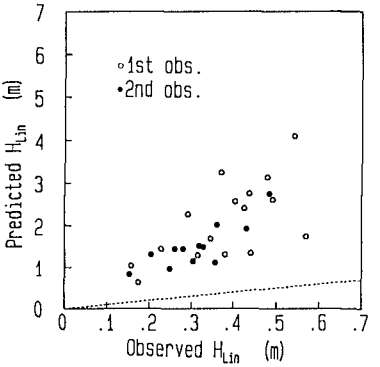

Figure 11 Comparison of observed infragravity wave height with predicted one (by the Symonds' model).

been considered to be caused by neglecting the travel time of small waves, because the conditions of their primary consideration χ=25–100 are far from our condition in the field observation. In the case of our condition, the trace of the break point has been extremely distorted sinusoidal curve, that is sawlike or overhanded, as shown with a solid line in Figure 10, even if the incident wave amplitude at the outside edge of the surf zone varies sinusoidally.

4.2 Modification of the Symonds' model

By taking the travel time into consideration, the Symonds' model must be modified. The position of the break point is given by

$$x_b = 1 + \Delta a \cos(t - t_b), \tag{14}$$

where Δa is a half width of dimension-less break point varying, t_b is the travel time required for a wave to propagate from x_2 to x_b(see Figure 10), which is written as

$$t_b = 2\sqrt{\chi}(\sqrt{x_2} - \sqrt{x_b}), \tag{15}$$

according to the shallow wave theory. The forcing term, F, can be expressed as a Fourier series as follows;

$$F(x,t) = \frac{1}{2x}\frac{\partial(a^2)}{\partial x} = 2\sum_{n=0}^{\infty}\{a_n(x)\cos nt + b_0(x)\sin nt\}, \tag{16}$$

$$a_0(x) = \frac{1}{4\pi}\int_{t_1(x)}^{t_2(x)} 1dt,\ b_n(x) = 0, \tag{17}$$

$$a_n(x) = \frac{1}{2\pi}\int_{t_1(x)}^{t_2(x)} \cos ntdt, \tag{18}$$

$$b_n(x) = \frac{1}{2\pi}\int_{t_1(x)}^{t_2(x)} \sin ntdt. \tag{19}$$

where $t_1(x)$ and $t_2(x)$ can be expressed with t_b defined by eq.(15) as follows:

$$t_1(x) = -\tau + t_b,\ t_2(x) = \tau + t_b,\ \tau = \arccos(\frac{x-1}{\Delta a}). \tag{20}$$

By substituting $t_1(x)$ and $t_2(x)$ into Eqs.(17),(18) and (19), we have

$$a_0(x) = \frac{\tau}{\pi}, \tag{21}$$

$$a_n(x) = \frac{\sin n\tau}{n\pi}\cos nt_b, \tag{22}$$

$$b_n(x) = \frac{\sin n\tau}{n\pi}\sin nt_b. \tag{23}$$

For the large value of χ, the travel time becomes long, being $t_b > \tau$. In this case, the trace of breaking point is overhanded, then $t_1(x)$ is given as

$$t_1(x) \doteq 0, \tag{24}$$

in place of Eq.(20). Under this condition, we also have a_0, a_n, b_n in the same way.

By combining Eqs.(10) and (11), the ζ_0 equation for $n = 0$, which is mean set-up, is simply given by

$$\zeta_0 = \begin{cases} -\frac{1}{\pi}\{(x-1)\tau - \sqrt{\Delta a^2 - (x-1)^2}\} & (x_1 < x < x_2) \\ \Delta a + (x_1 - x) & (0 < x < x_1) \end{cases} . \tag{25}$$

The ζ_n equations for $n >= 1$ is of the following form

$$\chi\frac{\partial^2\zeta_n}{\partial t^2} - x\frac{\partial\zeta_n}{\partial x} - \frac{\partial^2\zeta_n}{\partial x^2} = \begin{cases} \frac{\partial(2F_n x)}{\partial x} & (x_1 < x < x_2) \\ 0 & \text{otherwise} \end{cases} , \tag{26}$$

where

$$F_n = a_n(x)\cos nt + b_n(x)\sin nt. \tag{27}$$

If we put

$$\zeta_n = \frac{V_n(x)}{x^{1/2}}\exp(int), \tag{28}$$

and by substituting Eq.(28) into Eq.(26), we have

$$\exp(int)[\frac{\partial^2 V_n}{\partial x^2} + V_n(\frac{1}{4x^2} + \frac{\chi n^2}{x})] = \begin{cases} -\frac{1}{x^{1/2}}\frac{\partial(F_n x)}{\partial x} & (x_1 < x < x_2) \\ 0 & \text{otherwise} \end{cases} . \tag{29}$$

The homogeneous solution of Eq.(29) is given by

$$V_n = P_n x^{1/2} Z_0(Q_n x^{1/2}), \tag{30}$$

where Z_0 is the zero-th order Bessel function, J_0, or Neumann function, Y_0, $Q_n^2 = 4n^2\chi$.

Outside the forcing region, $0 < x < x_1$ and $x_2 < x$, the total solution is of the following form

$$\begin{aligned} \zeta_n &= \zeta_{nh}, \\ \zeta_{nh} &= \{A_n J_0(Q_n x^{1/2}) + B_n Y_0(Q_n x^{1/2})\}\cos nt \\ &+ \{C_n J_0(Q_n x^{1/2}) + D_n Y_0(Q_n x^{1/2})\}\sin nt, \end{aligned} \tag{31}$$

where A_n, B_n, C_n and D_n are the constants. In the forcing region, $x_1 < x < x_2$, the total solution is given by summing to following particular solution and eq.(31);

$$\begin{aligned} \zeta_n &= \zeta_{nh} + \zeta_{np}, \\ \zeta_{np} &= \{A_{np} J_0(Q_n x^{1/2}) + B_{np} Y_0(Q_n x^{1/2})\}\cos nt \\ &+ \{C_{np} J_0(Q_n x^{1/2}) + D_{np} Y_0(Q_n x^{1/2})\}\sin nt, \end{aligned} \tag{32}$$

$$A_{np} = -\pi[2a_n(x)xY_0(Q_nx^{1/2})]_{x_1}^{x} - \pi\int_{x_1}^{x} a_n(x)Q_nY_1(Q_nx^{1/2})dx,$$

$$B_{np} = \pi[2a_n(x)xJ_0(Q_nx^{1/2})]_{x_1}^{x} + \pi\int_{x_1}^{x} a_n(x)Q_nJ_1(Q_nx^{1/2})dx,$$

$$C_{np} = -\pi[2b_n(x)xY_0(Q_nx^{1/2})]_{x_1}^{x} - \pi\int_{x_1}^{x} b_n(x)Q_nY_1(Q_nx^{1/2})dx,$$

$$D_{np} = \pi[2b_n(x)xJ_0(Q_nx^{1/2})]_{x_1}^{x} + \pi\int_{x_1}^{x} b_n(x)Q_nJ_1(Q_nx^{1/2})dx,$$

where J_m is the m-th order Bessel function and Y_m is the m-th order Neumann function.

The constants are determined by setting the following conditions

at $x = 0$	with $\partial\zeta_n/\partial x = 0$,
at $x = x_1$ and $x = x_2$	with ζ_n and $\partial\zeta_n/\partial x$ continuous,
at $x = \infty$	with ζ_n outgoing progressive.

After all, the ζ solution is given by

$$\zeta = \sum_{n=0}^{\infty} \zeta_n. \tag{33}$$

Figure 12 shows the normalized amplitude at the shore line, which is calculated by the modified Symonds' model, as function of χ. In this figure, the results calculated by the original model are also shown with dotted lines. For χ smaller than 4, the modified model and the original model give the same results, while for χ greater than 4, the results predicted by the modified model is smaller than that of the original model. In the case of $n = 1$, the amplitude at the shoreline increases with χ up to $\chi = 15$, where the trace of break point begins to be overhanded, and it is decreases from here on.

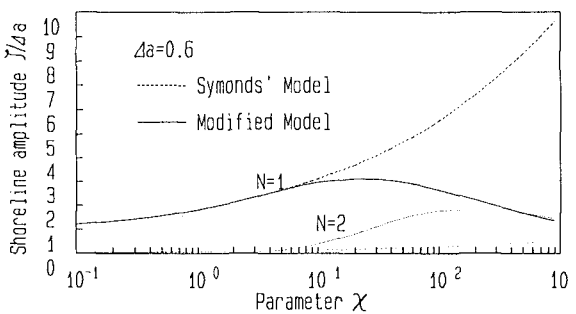

Figure 12 Normalized amplitude as a function of χ.

5 Verification of modified model with the field data

In the case of our field observation, as the value of χ is in range from 25 to 100, it is better to use the modified Symonds' model for estimating the height of infragravity waves in the surf zone. In the calculation, the assumptions described in the former section are employed, and the summation in Eq.(33) is conducted up to $n = 3$. Figure 13 shows the comparison of the observed infragravity wave heights in the surf zone with those predicted by the modified Symonds' model. Also in this case, the height of infragravity wave is the mean value of the heights

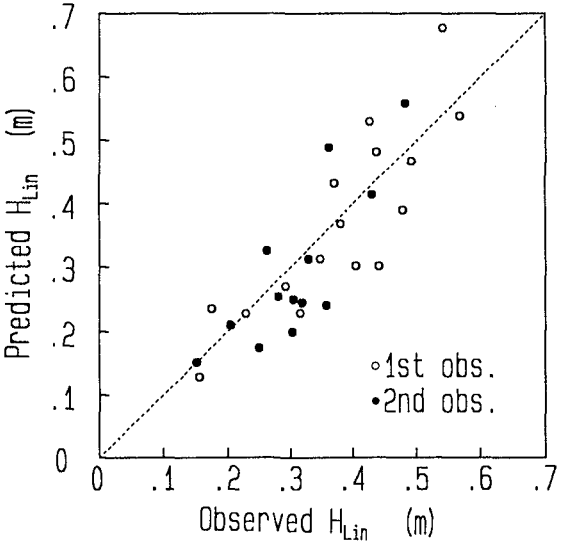

Figure 13 Comparison of observed infragravity wave height with predicted one(by the modified Symonds' model).

at the observation points in the surf zone. The data are plotted close to a dotted line, on which the observed height coincide with the predicted ones.

Next, let's do another verification of the modified Symonds' model. At the Port of Kashima located near the HORF, the waves and the currents are being permanently observed during 20 minutes of every two hours at the depth of about 24 meters. By utilizing these data, the value of ρ_{rms} and $\bar{T}_R$ were estimated by Eqs.(8) and (9) respectively, and the heights of infragravity waves in the surf zone have been predicted by the modified Symonds' model. In the HORF, the heights of infragravity wave have been measured at the point from No.1 to 7 throughout the year.

Figure 14 shows the comparison of the predicted heights of infragravity waves with the observed ones in the HORF during one year of 1989, where the comparisons are made for the data obtained at 12 o'clock of every day. There is a close agreement between them.

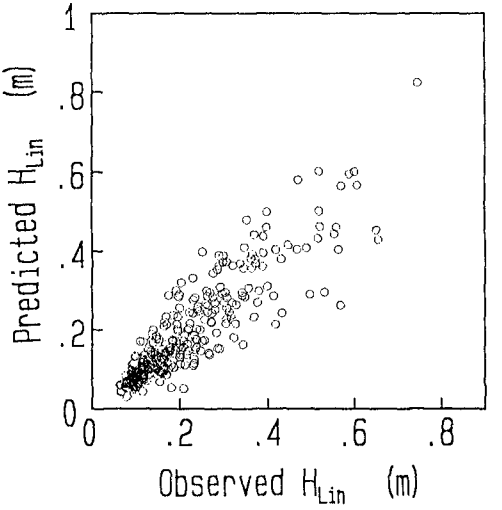

Figure 14 Comparison of predicted infragravity wave height by using the data of significant wave with observed one.

6 Conclusions

The main conclusions obtained in this study are as follows:

a) The period of wave groups, which is long in a deep sea during the storm, decreases in the process of wave breaking, and the infragravity waves become large in the surf zone.

b) The Symonds' theory has been modified by taking the effect of wave propagation into account. By means of this theory, the height of infragravity waves in the surf zone are estimated accurately with the representative value of wave groups, ρ_{rms} and $\bar{T}_R$.

c) Even if the data of significant waves are only available, the heights of infragravity waves could be estimated by using the theoretical and the empirical relationships between the significant waves and the wave groups.

References

Katoh,K and S.Yanagishima (1990):Berm Erosion Due to Long Period Waves, Proc. of 22nd ICCE, pp.2073-2086.

Katoh,K and S.Yanagishima (1992):Berm Formation and Berm Erosion, Proc. of 23rd ICCE.

Symonds,G., D.A.Huntley and A.J.Bowen (1982):Two-Dimensional Surf Beat: Long Wave Generation By a Time-Varying Breakpoint, J. Geophy. Res., Vol.87, No.C1, pp.492-498.

Goda,Y (1985):Random Seas and Design of Maritime Structures, University of Tokyo Press, 323p.

PART III

Coastal Structures

Pozzallo (*Sicily*)